Article

Defining the Landscape of the Pauling-Corey Rippled Sheet: An Orphaned Motif Finding New Homes

Jevgenij A. Raskatov,*,|| Joel P. Schneider,*,|| and Bradley L. Nilsson*,||

Read Online

ACCESS | Metrics & More | Article Recommendations

CONSPECTUS: When peptides are mixed with their mirror images in an equimolar ratio, two-dimensional periodic structural folds can form, in which extended peptide strands are arrayed with alternating chirality. The resultant topography class, termed the rippled β-sheet, was introduced as a theoretical concept by Pauling and Corey in 1953. Unlike other fundamental protein structural motifs identified around that time, including the α-helix and the pleated β-sheet, it took several decades before conclusive experimental data supporting the proposed rippled β-sheet motif were gained. Much of the key experimental evidence was provided over the course of the past decade through the concurrent efforts of our three laboratories. Studies that focused on developing new self-assembling hydrogel materials have shown that certain amphiphilic peptides form fibrils and hydrogel networks that are more rigid and have a higher thermodynamic stability when made from racemic peptide mixtures as opposed to pure enantiomers. Related interrogation of assemblies composed of mixtures of L- and D-amphiphilic peptides confirmed that the resulting fibrils were composed of alternating L/D peptides consistent with rippled β-sheets. It was also demonstrated that mirror-image amyloid beta (Aβ) could act as a molecular chaperone to promote oligomer-to-fibril conversion of the natural Aβ enantiomer, which was found to reduce Aβ neurotoxicity against different neuronal cell models. With a cross-disciplinary approach that combines experiment and theory, our three laboratories have demonstrated the unique biophysical, biochemical, and biological properties that arise upon mixing of peptide enantiomers, in consequence of rippled β-sheet formation. In this Account, we give an overview of the early history of the rippled β-sheet and provide a detailed structural description/definition of this motif relative to the pleated β-sheet. We then summarize the key findings, obtained on three unique sets of aggregating mirror-image peptide pairs through independent efforts of our three laboratories, and use these results to delineate the landscape of the rippled β-sheet structural motif to inspire future studies. Peptide sequence parameters that favor rippled β-sheet assembly are described, along with the accompanying kinetic and thermodynamic properties, as well as the resulting emergent physical properties of the assemblies. The Account then concludes with a brief overview of some key unresolved challenges in this nascent field. There is much potential for future applications of this unique supramolecular motif in the realm of materials design and biomedical research. We hope this Account will stimulate much-needed discussion of this fascinating structural class to eventually produce a fully quantitative, rational framework for the molecular engineering of rippled β-sheets in the future.
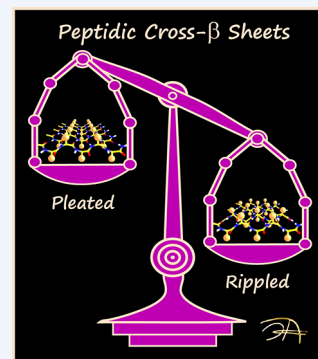
■ KEY REFERENCES

- Dutta, S.; Foley, A. R.; Warner, C. J. A.; Zhang, X.; Rolandi, M.; Abrams, B.; Raskatov, J. A. Suppression of Oligomer Formation and Formation of Non-Toxic Fibrils upon Addition of Mirror-Image Aβ42 to the Natural L-Enantiomer *Angew. Chem. Int. Ed.* **2017**, *56*, 11506–11510.[1]

  This paper reports on a strategy to promote an Aβ oligomer-to-fibril transition using a mirror-image peptide as the molecular chaperone. This effect, referred to as Aβ Chiral Inactivation, leads to a protection of neuronal model systems from Aβ neurotoxicity.

- Nagy, K. J.; Giano, M. C.; Jin, A.; Pochan, D. J.; Schneider, J. P. Enhanced Mechanical Rigidity of Hydrogels Formed from Enantiomeric Peptide Assemblies *J. Am. Chem. Soc.* **2011**, *133*, 14975–14977.[2]

  This paper was the first report describing that racemic mixtures of self-assembling peptides afford fibrillar gels that are more mechanically stiff than gels prepared from either enantiomer on their own.

- Swanekamp, R. J.; DiMaio, J. T. M.; Bowerman, C. J.; Nilsson, B. L. Coassembly of Enantiomeric Amphipathic Peptides into Amyloid-Inspired Rippled β-Sheet Fibrils *J. Am. Chem. Soc.* **2012**, *134*, 5556–5559.[3]

This paper confirmed the prediction that enantiomeric β-sheet peptides coassemble into Pauling rippled β-sheets with an alternating configuration of L/D peptides. This paper also demonstrated that the coassembly of racemic peptides mixtures into rippled β-sheets has a thermodynamic advantage over the self-assembly of single enantiomers into pleated β-sheets.

1. INTRODUCTION AND EARLY HISTORY

In the early 1950s, Pauling and Corey published three seminal papers in which they defined the β-sheet polypeptide structural motif. These studies were based on theoretical structural considerations and experimental X-ray diffraction data. The "pleated" β-sheet arrangement of peptides composed of canonical L-amino acids (AAs) was first reported in 1951.[4] The initially reported pleated β-sheet motif was renamed the "polar pleated" β-sheet in a subsequent publication later in 1951, in which the authors ironically stated that it was "unlikely [to be] an important configuration for proteins."[5] In this second paper, the authors introduced two new pleated β-sheet configurations, termed parallel-chain (i.e., parallel) and antiparallel-chain (i.e., antiparallel), respectively, reflecting the pairwise relative orientation of adjacent peptide strands in the sheet. In 1953, Pauling and Corey published their final paper on the pleated sheet, where they further refined the geometric parameters for parallel and antiparallel pleated sheets, and also introduced the concept of the "rippled" sheet.[6]

It is convenient to discuss the structure of the rippled β-sheet in comparison to the pleated β-sheet, a structural fold that is familiar to many readers. The pleated β-sheet can adopt either an antiparallel or a parallel configuration. In both cases, the constituent peptides adopt extended β-strand geometries that pack into β-sheets in which the α-carbons are aligned cross-strand in an "eclipsed"-like conformation as depicted in Figure 1A,B for a parallel pleated sheet. Adjacent rows of eclipsed Cα carbons are projected above and below the plane of the sheet in an alternating fashion. This gives the resulting β-sheet its characteristic pleated appearance. Figure 1A,C shows that, similarly to the Cα carbons, residue side chains are displayed from both faces of the β-sheet where they are aligned/eclipsed within each row along the long axis of the sheet.

The rippled β-sheet is made of L- and D-peptides arranged in an alternating L/D pattern. It is topographically distinct from the pleated β-sheet, as the opposite chirality of the alternating L- and D-peptide strands in the rippled sheet allows peptides to align such that the α-carbons between any two adjacent peptide strands are oriented to opposite faces of the rippled β-sheet (Figure 1D). Similar to its pleated counterpart, the rippled sheet can adopt either an antiparallel or a parallel configuration. Interestingly, in Pauling and Corey's original description of the rippled sheet, they never defined the ripple in the rippled sheet. That is, it is unclear what topographical feature of the sheet resembles the appearance of a ripple. Unlike the pleated sheet, where the pleats are easily described and visualized, ripples are not obvious. There appear to be two different topographical features that could have inspired the authors to introduce the term "rippled sheet". The first is the relative arrangement of Cα carbons with respect to the plane of the sheet. As one traverses the long axis of the β-sheet and traces a vector along a row of adjacent Cα carbon atoms, these atoms are positioned above and below the plane of the sheet in an alternating fashion, forming a ripple (Figure 1E). In contrast, the related carbons in a
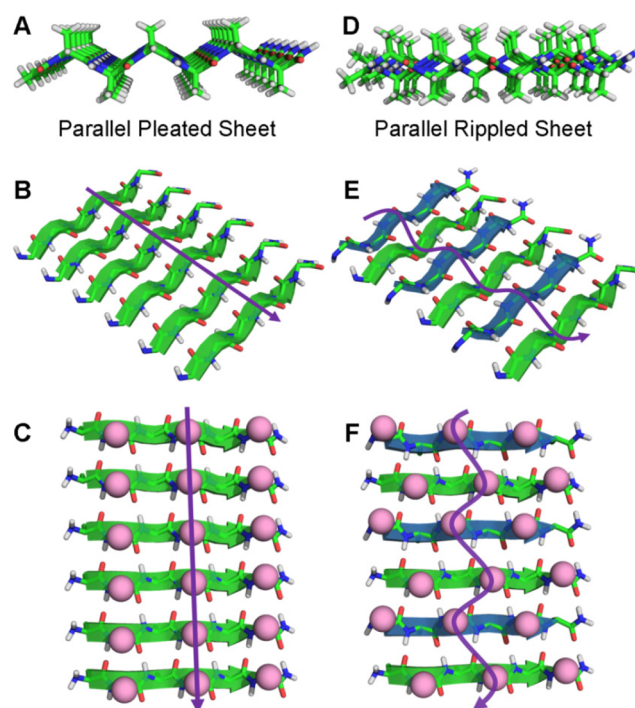
Figure 1. Parallel pleated sheet (A−C) and the parallel rippled sheet (D−F) in different projections. All-L peptide strands are green, and all-D peptides are blue; amino acid side chains are depicted as purple spheres in C (pleated, on a vertical line) and F (rippled, on a "waved" diagonal), leading to less steric repulsion. Similar steric requirements are obtained for the antiparallel sheets. The sheet twist is not shown in these idealized models, which were reconstructed using the Pauling-Corey coordinates.[6]

pleated sheet are all positioned either on the top or bottom of the sheet, depending on which row is viewed (Figure 1B). The second feature involves the placement of the residue side chains on either face of the sheet. In a rippled sheet, side-chain groups adopt a "staggered"-like cross-strand conformation within the sheet, orienting the side-chain groups in a zigzag configuration that could also be thought of as giving the sheet its rippled appearance (Figure 1F), contrasting the aligned arrangement of side chains within a pleated sheet (Figure 1C). Thus, there are two topographically distinct features that invoke the rippled nomenclature, and each may contribute to the unique properties of the rippled sheet, as discussed below.

The Pauling-Corey paper that introduced the rippled sheet in 1953 has been cited 291 times (Web of Science, 2020-08-11). However, most of the citing papers appear not to be related to rippled sheets. The term rippled is first noted in two back-to-back papers published by Lotz and co-workers in 1974. In studies combining electron diffraction and solid-state theory, the authors concluded that polyglycine I adopts a rippled and not a pleated antiparallel β-sheet structure.[7,8] This interpretation was later corroborated by Moore and Krimm through a vibrational analysis of polyglycine I.[9] A qualitatively similar rippled β-sheet was postulated in a later study that investigated peptide networks formed upon mixing of poly(L)- and poly(D)-β-benzyl-aspartate.[10] Similarly, precipitate formation, noted upon the mixing of poly(L)- with poly(D)-lysine, was ascribed to the formation of rippled sheets.[11] The L- and D-peptides that were used in the latter study were not of equal length, possibly due to matters of sample availability. The structure was termed polar pleated in the latter paper, which appears to be a misnomer, as

the authors drew an antiparallel rippled sheet as the proposed configuration, which would be more consistent with the experimental outcomes that they discussed. Later, Lahav and co-workers conducted insightful experiments to probe the mechanism of amino acid biochirogenesis, that is, breaking of mirror symmetry in the prebiotic world. Mass spectrometric evidence was provided for the preferential formation of rippled cross-β sheets in polymerization reactions of deuterium-tagged, activated valine or leucine racemic mixtures.[12] Similar mechanisms appear to operate with phenylalanine.[13] Interestingly, we also found valine, leucine, and phenylalanine are quite prone toward rippled sheet formation (vide infra). Aside from this handful of papers, very little work has been done on the rippled sheet, especially in comparison to the α-helix and the pleated β-sheet motifs.

2. RECENT ADVANCES

A systematic exploration of the rippled β-sheet as a novel supramolecular design principle was predominantly performed over the past decade by the three authors of this Account; our key advances, developments, and insights are discussed below.

2.1. Rippled β-Sheet Validation with Model Self-Assembling Peptides

In 2005, Goto et al. examined the influence of peptide chirality on the assembly of a fragment of the β_2-microglobulin protein.[14] They found that the L- and D-enantiomers of the 22-residue β_2-microglobulin K3 peptide (S20−K41) formed mirror-image twisted fibrils. Mixtures of the L- and D-K3 peptide also formed fibrils, although the L- and D-peptide content in these fibrils was not clear. They also observed that L-K3 fibril seeds only promoted the assembly of L-K3 monomer peptides and not the enantiomeric D-K3 monomers. Likewise, D-seeds only promoted the assembly of D-monomers. The authors concluded that a cross-reaction between the enantiomeric peptides was disfavored due to the instability of the resulting mixed β-sheet, thus refuting the prediction made by Pauling and Corey regarding rippled β-sheets.

This precedent inspired the Nilsson group to study whether mixtures of enantiomeric β-sheet peptides would self-sort to form mirror-image L- and D- pleated β-sheets, consistent with Goto's work, or if they would instead coassemble into rippled β-sheets as predicted by Pauling and Corey (Figure 2). In order to
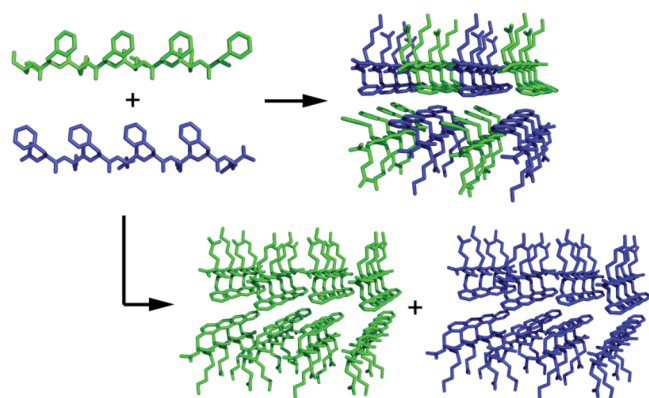
Figure 2. Schematic depiction of self-assembly of enantiomeric, amphiphilic KFE8 peptides (blue is L-Ac-(FKFE)$_2$-NH$_2$, green is D-Ac-(FKFE)$_2$-NH$_2$) into coassembled rippled β-sheet fibrils (top) or self-sorted enantiomeric fibrils (bottom). Reproduced with permission from ref 3. Copyright (2012) The American Chemical Society.

address this question, Nilsson adopted the KFE8 peptide (Ac-(FKFE)$_2$-NH$_2$) originally designed by Lauffenburger and co-workers.[15] KFE8 is a member of a class of amphiphilic peptides composed of alternating hydrophobic and hydrophilic amino acids that can assemble to form β-sheet bilayer nanofibrils, in which the hydrophobic side chains are sequestered in the interior of the bilayer structure.[15−18] Nanofibrils of the L-KFE8 peptide initially adopt a left-handed helical nanoribbon morphology.[16,19] The expectation was that the D-KFE8 peptide would assemble into mirror-image right-handed nanoribbons that should be easily differentiated from the left-handed fibrils of L-KFE8 if mixtures of L- and D-KFE8 were to self-sort into mirror-image pleated β-sheet nanoribbons formed by either exclusively all-L or all-D peptide.

Accordingly, the self-assembly of L- and D-KFE8 and mixtures of the enantiomeric peptides was examined.[3] As expected, solutions of L-KFE8 formed left-handed helical nanoribbons, and solutions of D-KFE8 formed right-handed helical nanoribbons (Figure 3). Interestingly, equimolar mixtures of L- and D-KFE8 did not produce mixtures of left- and right-handed nanoribbons but, instead, formed nonhelical tapelike nanofibrils. The unique morphology of fibrils, particularly the loss of twist in fibrils formed from racemic mixtures of L- and D-KFE8, was suggestive of a peptide coassembly into rippled β-sheets.

Several spectroscopic tools were used to confirm that racemic mixtures of KFE8 produced rippled β-sheets. First, fluorescence resonance energy transfer (FRET) was used to confirm that the fibrils contained both L- and D-KFE8. L-KFE8 and D-KFE8 were, respectively, labeled with donor and quencher molecules; the mixture of these peptides resulted in assemblies in which donor fluorescence was completely abrogated, consistent with coassembly of the peptides into mixed fibrils. Next, isotope-edited infrared (IE-IR) spectroscopy was used to confirm that the packing structure of the enantiomers within these mixed fibrils followed Pauling's predicted alternating L/D pattern for rippled β-sheets.[3] Selective carbonyl ^{13}C labeling of the L-KFE8 peptide indicated cross-strand coupling of the of the amide-1 IR absorption peak in the self-assembled pleated β-sheet fibrils. This coupling was lost when the labeled L-KFE8 peptide was coassembled with unlabeled D-KFE8. This observation provided clear evidence consistent with rippled β-sheet coassembly by L- and D-KFE8.

The relative thermodynamics of rippled versus pleated β-sheet assembly was examined using isothermal titration calorimetry (ITC) to gain insight in the mechanistic basis for rippled sheet formation by enantiomeric peptides (Figure 4).[3] Cationic and anionic derivatives of KFE8 were prepared: L-KF8 and D-KF8 (L- and D-Ac-(FK)$_4$-NH$_2$) and L-EF8 (L-Ac-(FE)$_4$-NH$_2$). These peptides fail to self-assemble due to charge repulsion. However, equimolar mixtures of KF8 and EF8 coassemble due to charge complementarity. These properties enabled the use of these peptides in ITC experiments in which L-EF8 was mixed with either L-KF8 (to form pleated β-sheets) or D-KF8 (to form rippled β-sheets). The formation of the rippled β-sheets was thermodynamically preferred with an enthalpic advantage of ~9 kcal mol^{-1} relative to the pleated β-sheet formation. The structural basis for this enthalpic advantage is not yet understood, but it could be due to differences in the cross-strand packing structure for rippled versus pleated β-sheets.

The emergent properties of pleated (formed by enantiopure L-KFE8) and rippled β-sheets (formed by an equimolar mixture
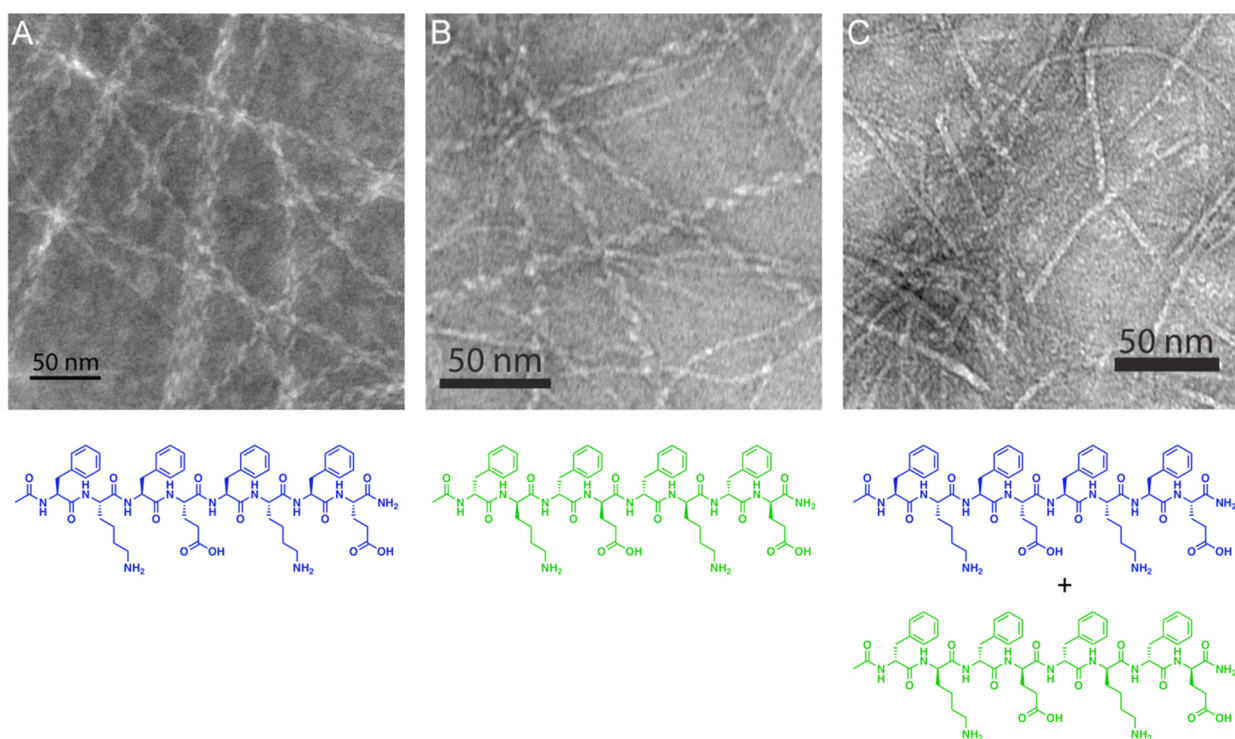
Figure 3. (A) TEM image of left-handed helical nanoribbons of L-Ac-(FKFE)$_2$-NH$_2$ pleated β-sheets; (B) TEM image of right-handed helical nanoribbons of L-Ac-(FKFE)$_2$-NH$_2$ pleated β-sheets; (C) TEM image of nonhelical nanoribbons of coassembled L/D-Ac-(FKFE)$_2$-NH$_2$ rippled β-sheets. Reproduced with permission from ref 3. Copyright (2012) The American Chemical Society.

of L-KFE8 and D-KFE8) were also compared.[20] Fibrils resulting from the assembly of these peptides can form hydrogel networks. Consistent with the findings of the Schneider group with their MAX peptides (see Section 2.2), rippled β-sheet nanofibrils of L- and D-KFE8 formed more rigid viscoelastic hydrogel networks than the corresponding all-L or all-D pleated β-sheet networks. Also, while the all-L pleated β-sheet fibrils of KFE8 were completely degraded by trypsin, chymotrypsin, and proteinase K within 5 d, L/D rippled β-sheets of KFE8 were stable to degradation over the same time period. These findings illustrate the unique properties of rippled β-sheets compared to pleated β-sheets and are suggestive of novel applications for rippled β-sheets as biomaterials.

The KFE8 peptide and the Schneider MAX peptides (see Section 2.2) that have been shown to form rippled β-sheets share common sequence patterns of alternating hydrophobic/hydrophilic amino acids. The amyloid β 16–22 fragment (Aβ(16–22), Ac-KLVFFAE-NH$_2$) was used to determine whether a broader scope of peptide sequence patterns assemble into rippled β-sheets.[21] Equimolar mixtures of L- and D-Aβ(16–22) aggregated at dramatically accelerated rates compared to solutions of either enantiomer alone.[21] In addition, the putative rippled β-sheet L/D assemblies adopted a needlelike, pseudocrystalline appearance, while the L- or D-pleated β-sheets were twisted fibrils. IE-IR studies confirmed the L/D alternating packing arrangement that characterizes rippled β-sheets. Solid-state NMR (SSNMR) was used to determine ^{19}F–^{13}C distance correlations within these mixed fibrils that further confirmed a rippled β-sheet architecture that agreed with a predicted cross-strand packing model (Figure 5). As with KFE8, a rippled β-sheet coassembly of L- and D-Aβ(16–22) was found to be enthalpically favorable to pleated β-sheet assembly by ~2 kcal mol^{-1} as determined by sedimentation analysis. A

sedimentation analysis involves a quantification of monomer concentration in a self-assembly mixture over time by the separation of aggregates from monomeric peptide by ultracentrifugation. The monomer concentration at equilibrium can be used to extrapolate equilibrium constants and comparative free energies of self-assembly reactions. These findings suggest that the coassembly of enantiomeric β-sheet peptides into L/D patterned rippled β-sheets may be general, regardless of sequence pattern.

2.2. Rippled Sheets from Self-Assembled β-Hairpins

Schneider et al. happened upon the rippled β-sheet while designing hydrogels formed from self-assembling β-hairpin peptides. These peptides are designed to undergo triggered self-assembly into β-sheet-rich fibrils that become physically cross-linked, forming moderately stiff hydrogels.[22–25] If therapeutic small molecules,[26] proteins,[27–29] nucleic acids,[30] liposomes,[31] or even cells[32–34] are present during self-assembly, they get directly encapsulated into the gel network. The gels can be syringe-injected to tissue, where they locally deliver their payload.[35,36] The sequence of one particular peptide, called MAX1, is shown in Figure 6A.

Molecular chirality is a useful design tool in fabricating hydrogel materials.[37–39] For example, the proteolytic susceptibility of the MAX1 gel can be regulated by doping increasing amounts of the enantiomeric peptide, DMAX1, into the gel formulation. As increasing amounts of DMAX1 are added, both the degree and the rate of degradation are attenuated, Figure 6B. While studying the rheological properties of these gels an unexpected and puzzling observation was made. Figure 6C shows that gels prepared from enantiomeric mixtures are characterized by nonadditive, synergistic enhancements in their mechanical rigidities compared to hydrogels prepared from either pure MAX1 or DMAX1 peptides alone.[2] The racemic gel
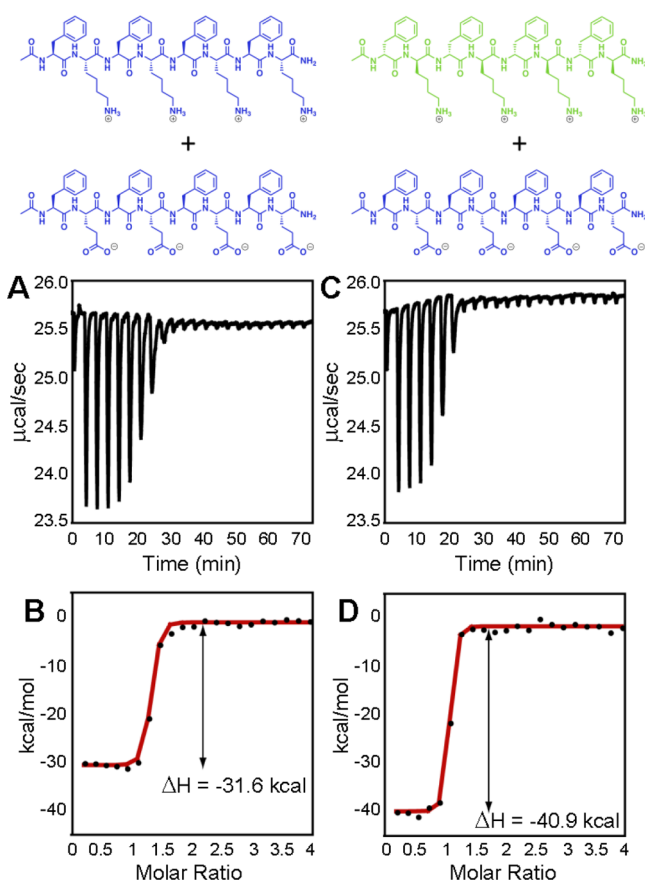
Figure 4. Representative raw (A) and fit (B) ITC data for the injection of L-KF8 into L-EF8, and representative raw (C) and fit (D) ITC data for the injection of D-KF8 into L-EF8. Reproduced with permission from ref 3. Copyright (2012) The American Chemical Society.

displays the greatest enhancement in storage modulus (G', a measure of mechanical stiffness). Keeping in mind that each 1 wt % gel contains the same number of peptides capable of assembly, the racemic gel's fourfold enhancement in rigidity is amazing and possibly represented a new paradigm in materials design if one could understand its origin. This observation sparked a five-year quest to uncover the molecular, local, and network-level basis for the enhanced gel stiffness that ended at the doorstep of Pauling and Corey's prediction of the rippled β-sheet.[6]

Pure MAX1 gels are prepared by initially dissolving the peptide in water, where it remains monomeric and unstructured, until its assembly is triggered by adjusting the solution pH, ionic strength, and/or temperature. Solid-state NMR shows that MAX1 assembles with high fidelity into monomorphic fibrils, where it is folded into a well-defined β-hairpin conformation (Figure 7A).[40] Fibrils are composed of a bilayer of hairpins that hydrogen bond along the fibril's long axis. The bilayer is formed by the association of the hairpins' valine-rich faces, which shields these hydrophobic side chains from water (Figure 7B).[41] Hairpins adopt a *syn*-arrangement within each monolayer having their β-turns on one side of the fibril but adopt an *anti*-arrangement relative to hairpins across the bilayer. With respect to the racemic mixture, transmission electron microscopy (TEM) and fluorescence experiments showed that enantiomers coassembled into mixed fibrils as opposed to self-sorting to form enantiomeric pure fibrils (Figure 8).[42] Thus, it was hypothesized that interactions made between enantiomers in the fibrillar state

might be the basis for the observed enhancement of the racemic gel's rigidity.

Polymer theory predicts that the mechanical rigidity (G', storage modulus) of a semiflexible network depends on two adjustable parameters, namely, the fibril bending modulus (κ) and the mesh size (ξ) of the fibril network according to the equation $G' = \kappa^2/kT\xi^5$, where k and T are the Boltzmann constant and temperature.[43−45] So, changes in either the mesh size and/or the fibril bending modulus are responsible for the enhancement in gel rigidity. The mesh size is directly related to the number of cross-links in the fibrillar network. More cross-links lead to a smaller mesh size and, correspondingly, a stiffer gel. The bending modulus (κ) describes the mechanical stiffness of individual fibers in the gel network. Stiffer fibrils lead to more rigid gels. Small-angle neutron scattering (SANS) ruled out that changes in mesh size were at play, whereas diffusing wave spectroscopy (DWS) conclusively showed that fibrils formed from the coassembly of MAX1 and DMAX1 enantiomers were more stiff than fibrils formed from either pure peptide.[42] Thus, the racemic hydrogel is more rigid than the gel made from either of the pure enantiomers, because the individual racemic fibrils are stiffer.

Molecular interactions between MAX1 and DMAX1 are most likely responsible for the enhanced stiffness of the racemic fibrils. Solid-state NMR, isotope-edited Fourier transform infrared (FTIR) spectroscopies, and computation led to the molecular model depicted in Figure 8 (at right). Here, the MAX1 and DMAX1 enantiomers coassemble in alternating fashion along the long axis of the fiber (only eight hairpins are shown). Unlike pure MAX1 fibrils, the enantiomers are arranged with an antiorientation within each monolayer. Similar to MAX1 fibrils, the hairpins adopt an antiarrangement across the bilayer. The alternating arrangement of enantiomers along each monolayer forms a rippled β-sheet using β-hairpins as opposed to single β-strands. Figure 9A shows two β-hairpins excised from a racemic fibril monolayer. Their antiarrangement allows the formation of an intermolecular, stereochemically mixed two-stranded parallel sheet (one D-strand and one L-strand highlighted in yellow) with bent intermolecular H-bonds. Rotating this model by 90° allows one to see the rippled arrangement of Cα atoms. For comparison, Figure 9B shows the Pauling-Corey model of a parallel rippled sheet, where two β-strands form a series of bent intermolecular H-bonds with the same rippled arrangement of Cα carbons. The models in Figure 9C suggest that the molecular origins leading to an enhanced stiffness for the rippled fibril involves the energetically favorable packing of valine side chains within the fibril's core. The rippled sheet allows their staggered arrangement, where the entire isopropyl group of one valine nestles between the isopropyl groups of its valine neighbors across the sheet. This allows tight packing that maximizes side-chain/side-chain van der Waals interactions, stabilizing the fiber's hydrophobic core. Nested hydrophobic interactions such as these are observed in the structures of naturally occurring β-sheet proteins, where they stabilize the folded state.[46] In contrast, the valine side chains within the enantiomeric pure MAX1 fibrils interact in a head-to-head fashion, which does not pack the interior of the fibril as efficiently as the nested arrangement. Thus, the well-packed interior of the racemic fibrils, with their nested valine side chains, results in their local stiffening, which in turn, is responsible for the increased mechanical rigidity observed for the racemic gel.
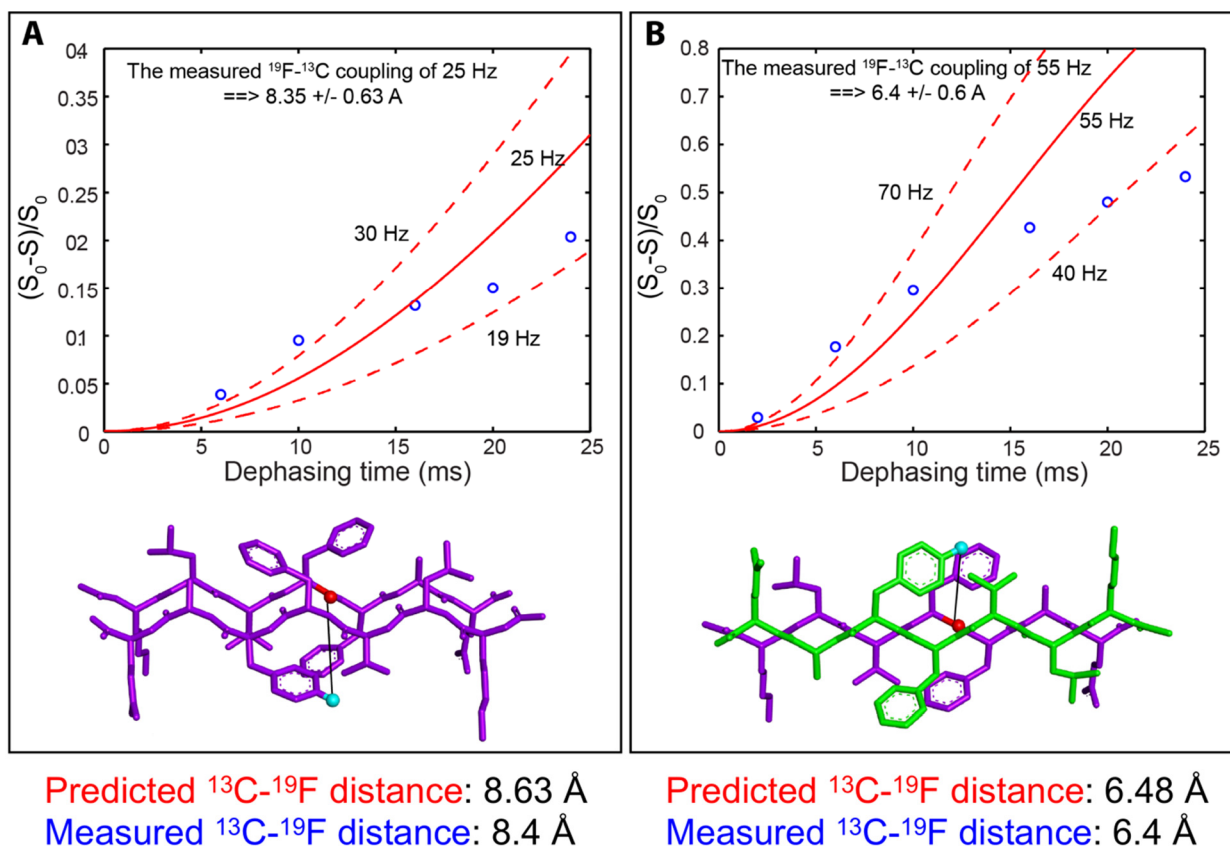
Figure 5. (A) Dephasing curve used to determine the 1-^{13}C to ^{19}F distance in pleated β-sheet cofibrils of L-Ac-KLV**F**FAE-NH$_2$ with L-Ac-KLVF(4-F-Phe)AE-NH$_2$ (purple). A predictive model for the cross-strand β-sheet orientation of these peptides is shown with the 1-^{13}C (red) and ^{19}F (cyan) labels indicated. (B) Dephasing curve used to determine the 1-^{13}C to ^{19}F distance in rippled β-sheet cofibrils of L-Ac-KLV**F**FAE-NH$_2$ with D-Ac-KLVF(4-F-Phe)AE-NH$_2$ (green). A predictive model for the cross-strand orientation of these peptides in rippled β-sheets is shown with the 1-^{13}C (red) and the ^{19}F (cyan) labels indicated. Reproduced with permission from ref 21. Copyright The Authors, some rights reserved; exclusive licensee MDPI. Distributed under a Creative Commons Attribution License 4.0 (CC BY) https://creativecommons.org/licenses/by/4.0/.
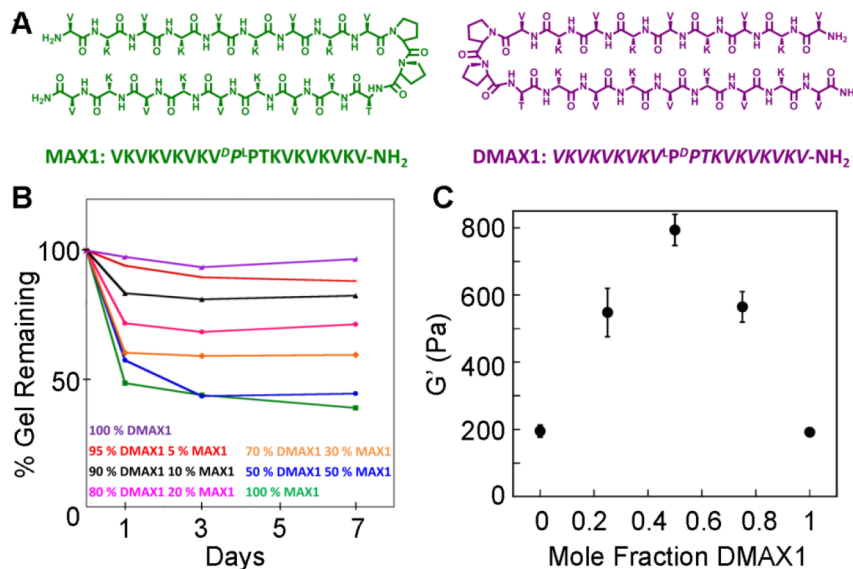
Figure 6. (A) Sequences of MAX1 (green) and its enantiomer DMAX1 (purple). (B) Adding increasing amounts of DMAX1 into the MAX1 gel formulation retards proteolysis. (C) Hydrogel storage modulus G' measured as a function of mole fraction of DMAX1 in a background of MAX1. The gel is stiffest when an equimolar (racemic) mixture of MAX1 and DMAX1 is used for its preparation. Reproduced with permission from ref 2. Copyright (2011) The American Chemical Society.
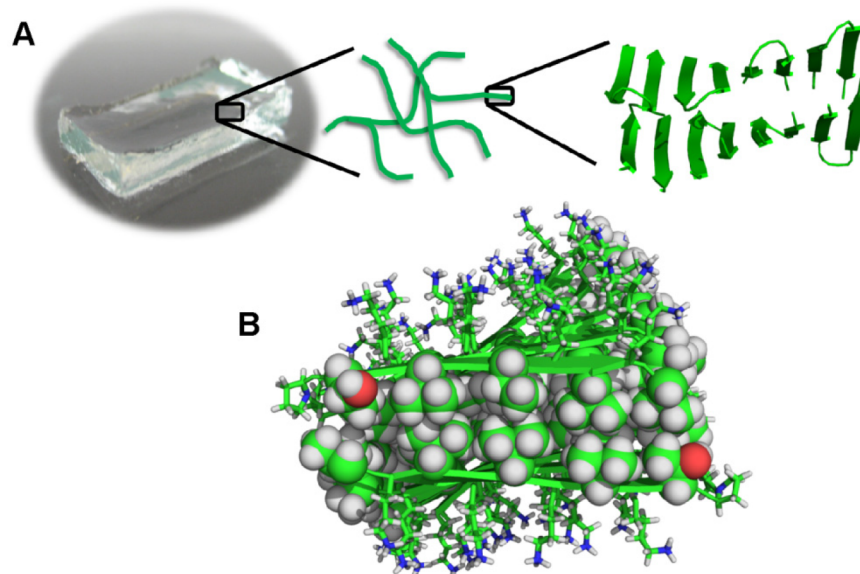
Figure 7. (A) Image of MAX1 hydrogel and a schematic of its underlying fibril network. Solid-state NMR-based structure of the hairpins in their self-assembled state; (B) an axial view looking down the long axis of a fibril showing the packing of the valine side chains (CPK rendering) in the interior of the fibril's bilayer.
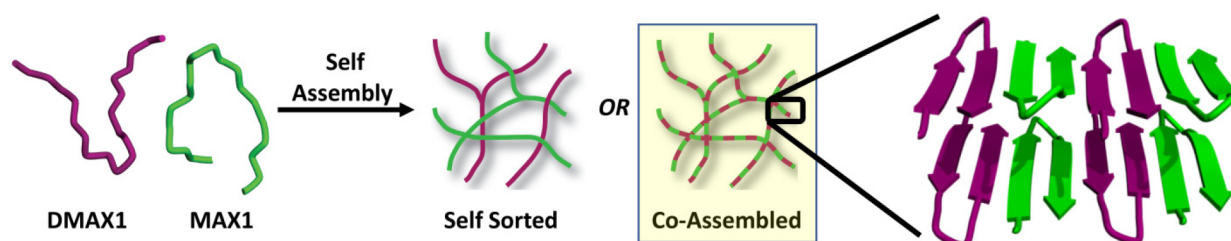
Figure 8. A segment of the coassembled rippled β-sheet formed from an equimolar mixture of MAX1 and DMAX1. The structural model was derived from solid-state NMR, isotope-edited FTIR, and computation.

2.3. Rippled Sheets in Amyloid β Chiral Inactivation

Amyloid β chiral inactivation (Aβ-CI) was developed by the Raskatov lab as a molecular method to stimulate Aβ oligomer-to-fibril conversion to suppress peptide neurotoxicity, using mirror-image Aβ as the molecular chaperone.[1,47,48] The approach was inspired by two seemingly unrelated insights:

1 From Crystals to Amyloids: The Stereochemical Foundation of Aβ-CI.

   Racemates have a higher crystallization propensity than enantiomers. This seems counterintuitive at first: why should compounds crystallize better from equimolar enantiomer mixtures? The answer comes from space-group statistics. From the total of 230 space groups, only 65 can be populated through pure enantiomers, as the other 165 contain inversion elements and need both mirror-image molecules to generate the lattice.[47] Because of that, racemates are some 10-fold more likely to crystallize than pure enantiomers.[49] This phenomenon proved beneficial for Raskatov et al. in their structure–function studies of asymmetric catalysts. Frequently, racemates would form crystals, under conditions where pure enantiomers formed oils.[50,51]

2 The Aβ Aggregation-Toxicity Relationship.

   Aβ is an important actor of Alzheimer's disease (AD).[52,53] This peptide may adopt different conformational and aggregated states, often with vastly different properties.[54−59] In 2010, Aβ oligomer-to-fibril conversion was shown to suppress Aβ neurotoxicity,[60] suggesting that Aβ fibrils may act as a protective reservoir that scavenges the more toxic Aβ forms.

Aβ oligomers are dynamic and largely unordered, which may be considered an oil-like behavior, whereas Aβ fibrils have a long-range periodicity in the z-dimension and can, therefore, be thought of as crystal-like (Figure 10). On the basis of arguments presented under #1 (aforementioned), Raskatov hypothesized mirror-image ("D-"; "all-D") Aβ should promote Aβ oligomer-to-fibril conversion. On the basis of arguments presented under #2, it was further hypothesized this conversion should suppress Aβ toxicity.[47] The approach was buttressed through studies by Nilsson and Schneider (see Sections 2.1 and 2.2), published around that time.[2,3]

Aggregating peptides are challenging to study. A wide array of techniques is required to understand the molecular processes. The first study by the Raskatov lab focused predominantly on Aβ42, which is more aggregation-prone and more toxic than the more prevalent, two amino acid shorter, Aβ40.[56] L- and D-Aβ42 were synthesized, and their fibril formation kinetics were measured using the Thioflavin T (ThT) fibril formation assay. As expected, L- and D-Aβ42 displayed lag phases of comparable duration, as well as very similar fibrillization $t_{1/2}$ and final fluorescence values.[1] A mixing of the enantiomers led to the disappearance of the lag phase (Figure 11, left). The fibrillization
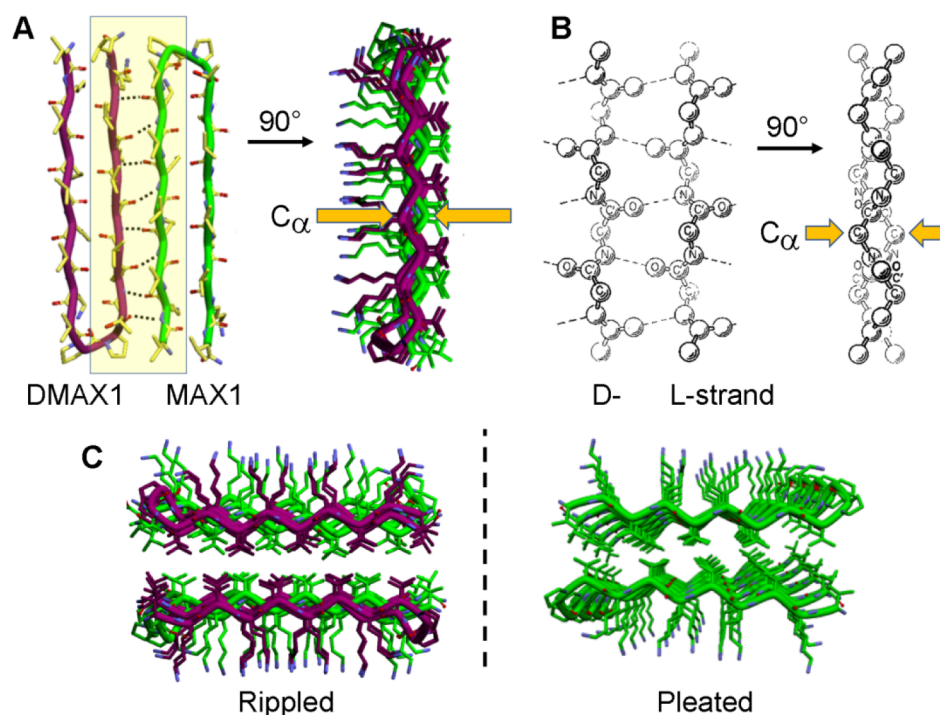
Figure 9. (A) DMAX1:MAX1 dimer excised from a racemic fibril monolayer. (B) The original Pauling-Corey model of the rippled parallel β-sheet. Both are shown in two orthogonal projections, and Cα carbons are indicated with arrows. (C) Comparison of valine side-chain packing within the hydrophobic cores of the rippled vs pleated β-sheet fibrils.
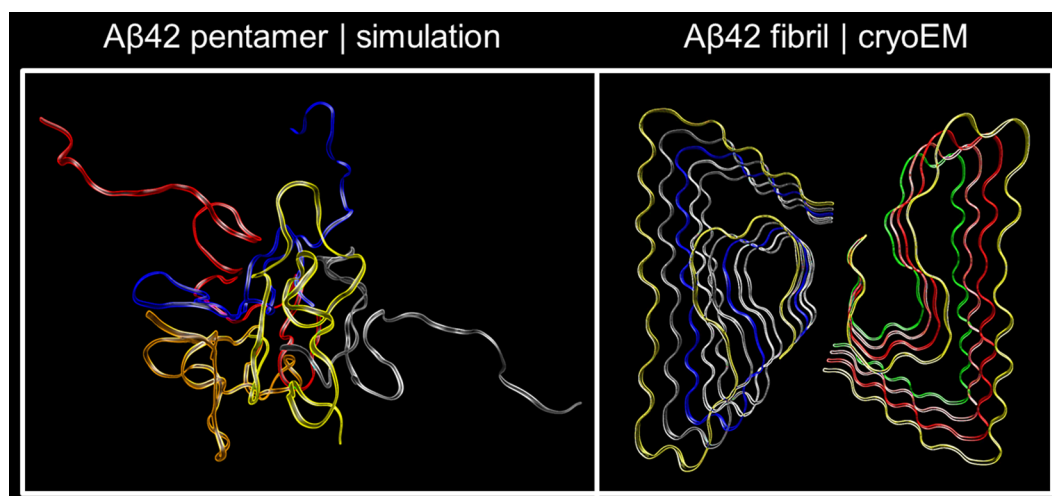

Figure 10. (left) An Aβ42 pentamer from an MD simulation.[61] (right) An Aβ42 cryoEM fibril structure.[62] Structures rendered from coordinates that are either published (cryoEM fibril) or were generously provided by Dr. Urbanc (pentamer simulation).

$t_{1/2}$ and final fluorescence values were also lower, indicating fibrils formed were structurally distinct. Similar trends were later observed with the Aβ40 system (Figure 11, right).[63] Fibrils from racemic Aβ40 and Aβ42 had unique morphologies. Enantiopure Aβ40 was approximately twofold wider than the racemic, and it was twisted, whereas the racemic was flat.[63] With Aβ42 the racemic fibrils tended to be longer, less clumped, and more threadlike than enantiopure. This is consistent with the study of the KLVFFAE model peptide by Nilsson and co-workers.[21]

In subsequent gel electrophoretic experiments that measure Aβ42 aggregation intermediates Aβ42 enantiomer mixing led to the elimination of soluble Aβ oligomers (Figure 12A). This protected neuronal model cells from Aβ42 toxicity, presumably by removing the most toxic Aβ species from solution.[1] ^{1}H NMR

was used as an orthogonal technique to monitor changes in solubility upon Aβ40 enantiomer mixing.[63] L-Aβ40 could be monitored without changes in the ^{1}H NMR signal strength (Figure 12B), which was used as a proxy for concentration of soluble Aβ. The addition of 1 equiv of D-Aβ40 triggered the precipitation of soluble Aβ, leading to a loss of more than 60% soluble Aβ signal in ~40 min (Figure 12C). Similarly to the Nilsson and the Schneider systems, Aβ-CI is believed to operate via a rippled β-sheets formation.

The LVFF central hydrophobic segment of Aβ is known to be of high importance for Aβ fibrillization.[64] As discussed in Section 2.1, Nilsson and co-workers found that mixing of the KLVFFAE peptide with the mirror-image klvffae peptide lowered the system solubility, consistent with trends by
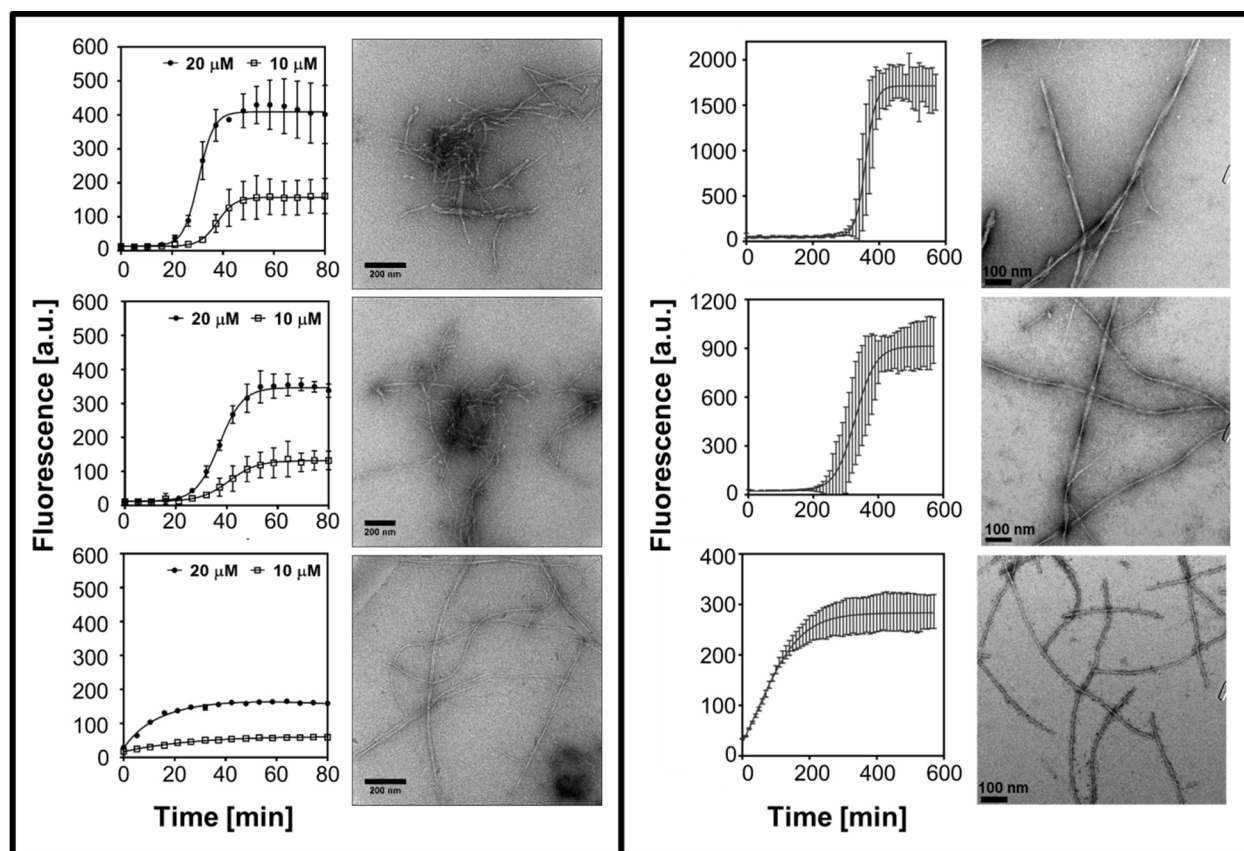
Figure 11. (left panels) ThT fibril formation kinetic curves for Aβ42; fibrils imaged at end point by TEM; scale bars: 200 nm. (top) L-Aβ42, (middle) D-Aβ42, (bottom) racemic Aβ42. (right panels) ThT fibril formation kinetic curves for Aβ40; fibrils imaged at end point by TEM; scale bars: 100 nm. (top) L-Aβ40, (middle) D-Aβ40, (bottom) racemic Aβ40. Reproduced with permission from ref 1. Copyright (2017) Wiley-VCH.
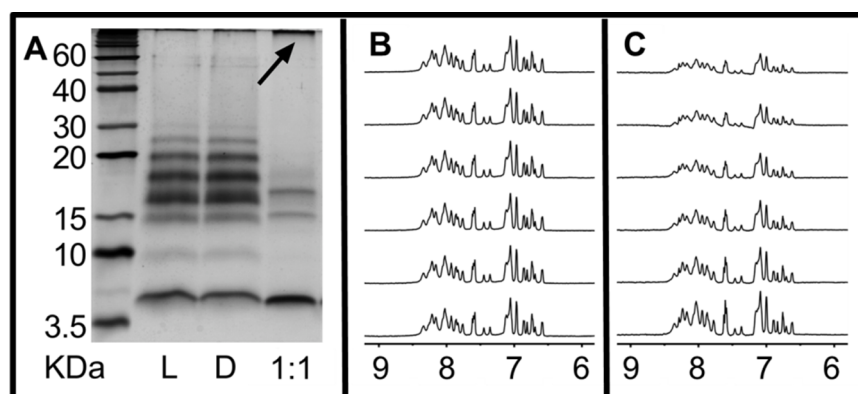

Figure 12. (A) Photo-cross-linked L-, D-, and racemic Aβ42 separated by gel electrophoresis. (B) Monitoring of L-Aβ40 by ^{1}H NMR shows no changes in concentration over ca. 40 min (bottom to top). (C) Mixing of L- and D-Aβ40 in a 1:1 ratio triggers precipitation, with ~60% ^{1}H NMR signal loss over the same 40 min (bottom to top). Reproduced with permission from ref 1, copyright (2017) Wiley-VCH, and from ref 63, copyright (2019) Wiley-VCH.

Raskatov et al.[21] Intriguingly, the short Aβ-derived mirror-image tetrapeptide, lvff, inhibits Aβ aggregation by binding to the central hydrophobic cluster of Aβ.[65] This shows that more than just the central hydrophobic region is needed for Aβ-CI to operate.

To gain deeper, molecular level insights, density functional theory (DFT) quantum-chemical calculations were performed.[63,66,67] With the Pauling-Corey coordinates as a starting point, diverse LVFFA:lvffa rippled dimers were generated. One of those structures was found to be more stable than LVFFA:LVFFA homochiral dimers from three published Aβ

fibril structures.[66] Since then, Raskatov found a rippled antiparallel cross-β LVFFA:lvffa dimer that is even more stable (Figure 13). Energetics may be different for more extended sheets.[67] DFT calculations conducted thus far only model the isolated LVFFA fragment, not taking into account that there are other segments within Aβ that may also form rippled interfaces, which may bias the system toward the parallel rippled sheet or other structures. Future experimental work may provide more conclusive structural information on Aβ-CI fibrils. Also, more work is needed to better understand the thermodynamic and kinetic effects that govern the formation of rippled sheets in
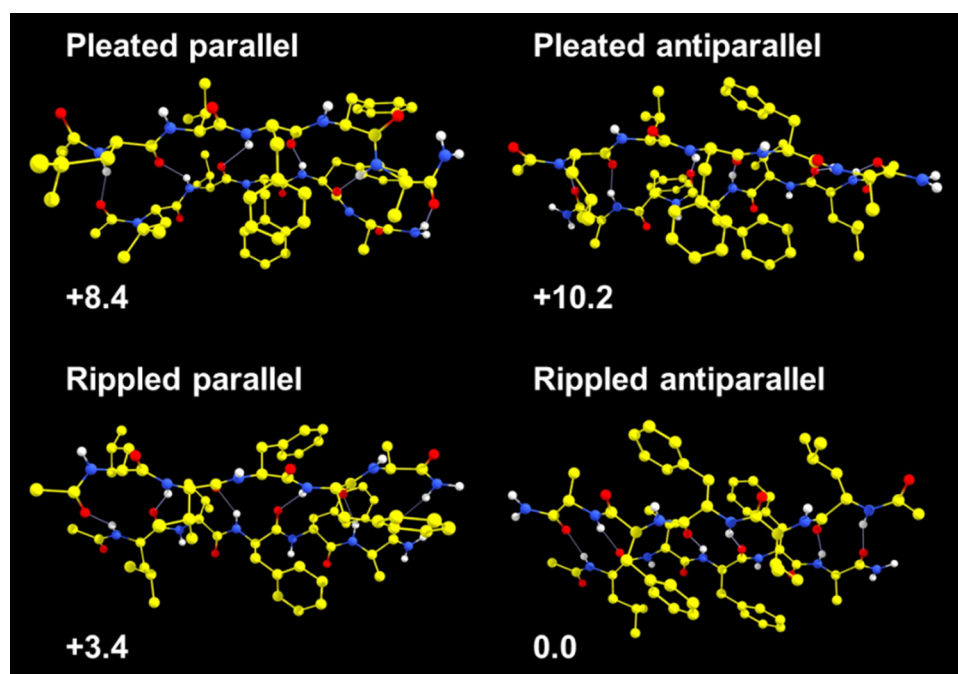
Figure 13. Pleated parallel dimer was obtained from the Aβ42 structure (5oqv),[62] and the pleated antiparallel was obtained from the Aβ40-D23N structure (2lnq).[68] The antiparallel structures were built from Pauling-Corey coordinates, and all four structures were N-terminally acetylated and C-terminally amidated, and fully geometry-optimized as described previously.[63,66,67,69]

general, as the mechanism of Aβ-CI may be transferrable to other intrinsically disordered peptides, such as amylin, as well as other chemically similar systems.[53]

## 3. KINETICS, THERMODYNAMICS, AND UNRESOLVED CHALLENGES

The work from our groups transposes the rippled β-sheet from a theoretical concept to an experimentally established supramolecular motif. However, much work is still needed. For example, decades of studies have defined the structure, thermodynamics, and kinetics of pleated β-sheet folding. These data, which are essential to our understanding of peptide and protein folding, misfolding, and aggregation behavior, have yet to be collected for rippled sheets.

Data hinting that rippled sheets behave differently are just now becoming available. Our laboratories, working with different peptide sequences, have observed that fibrils prepared from racemic mixtures form faster than the corresponding enantiopure systems. For example, Figure 14A shows the fibrillization kinetics for the Aβ42 peptide performed by the Raskatov lab. Enantiomerically pure solutions of L- or D-Aβ42 display a characteristic lag phase and similar elongation phases. In sharp contrast, the racemic mixture shows no observable lag phase and an extremely fast rate of assembly leading to fiber formation. Using enantiomers of Aβ(16−22), Nilsson's lab showed that rippled sheet assembly reaches equilibrium within 2 h, while it takes the pleated sheet longer than 3 d to come to equilibrium (Figure 14B).[21] Solutions become turbid as fibrils are formed for this system. The inset qualitatively shows that the racemic mixture is turning turbid at 30 min, whereas pure L-Aβ(16−22) remains nearly clear. Figure 14C shows a time-sweep rheology experiment from Schneider's lab measuring the evolution of gel rigidity by assembling MAX1 and DMAX peptides. In addition to the racemic gel comprised of rippled

fibrils being mechanically stiffer than the enantiomerically pure gels, its initial rate of formation is faster.

Taken together, the data from Figure 14A−C suggest that the activation energy that leads to rippled β-sheet fibrils is lower than that leading to pleated sheets. This is schematized in a proposed energy diagram in Figure 14D. Our understanding of the mechanism(s) leading to the formation of rippled sheet fibrils is sparse but might have similar features to amyloid fibril formation for which much work has been done.[70] For example, the formation of rippled fibrils is likely under kinetic control. The energy landscapes may be rugged and characterized by thermodynamically disfavored nucleation events en route to the transition state followed by a rapid energetically favorable elongation phase.[71] The energy associated with traversing $\Delta G_{L/D}^{\ddagger}$ likely encumbers the stripping of water from polar hydrogen-bond donors and acceptors, as new H-bonds are formed during assembly, and the fixing of dihedral angles associated with conformational rearrangements to form a critical nucleus capable of fibril formation.[72] Primary nucleation, during the lag phase, may involve the formation of multimeric assemblies (oligomers) that could be on-pathway intermediates or off-pathway reversible or irreversible sinks.[73] Nucleation can also be secondary in nature, where new fibril growth is catalyzed at the surface of already-formed fibrils.[74] All of this is further complicated by the possible formation of enantiomerically pure and/or mixed intermediates and nuclei. Once a competent nucleus is formed, elongation should be energetically downhill, most likely characterized by monomer addition,[75] or even preformed segments to the growing fibril with the complicating factors of strand registry, direction (parallel vs antiparallel), and mirror-image pairing.[76] In addition, conformational selection has recently been proposed to accelerate fibril formation upon enantiomer mixing;[66] future research may reveal other underlying reasons for this fascinating effect.
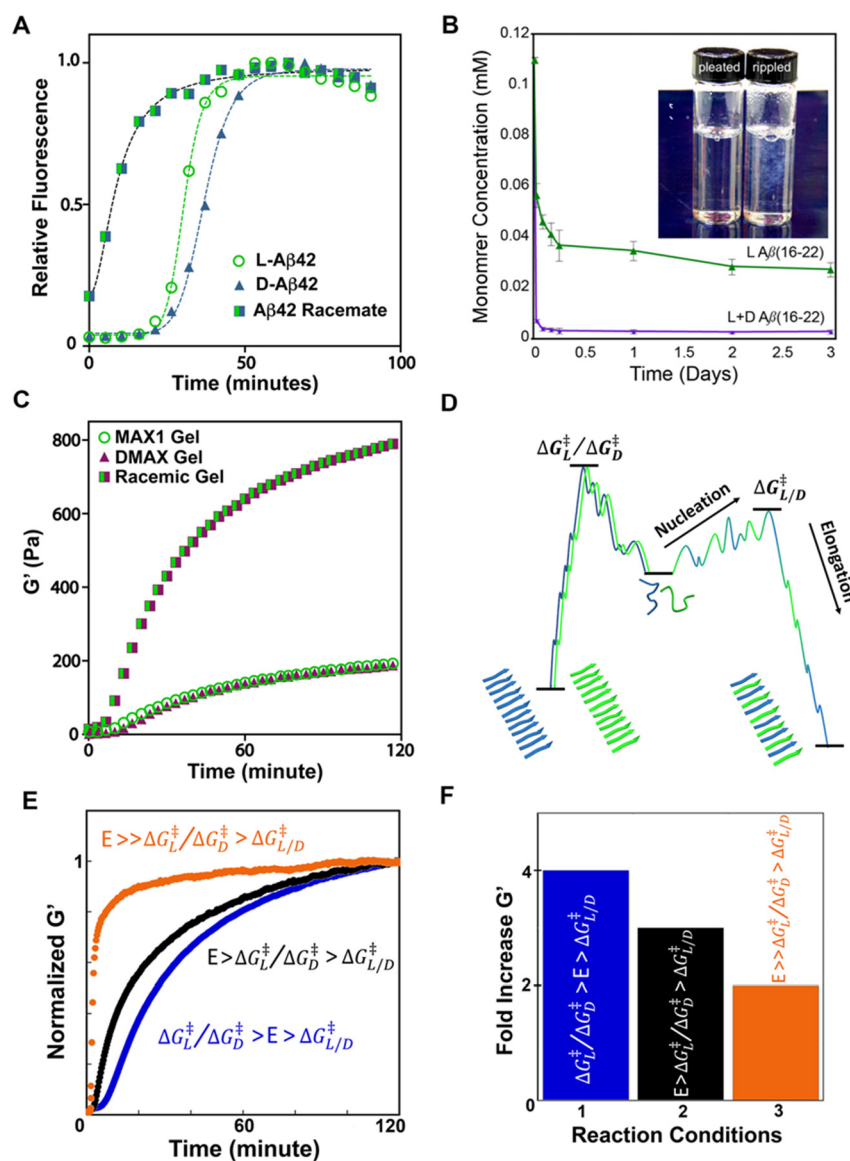
Figure 14. (A) Kinetics of fibril formation for enantiopure or racemic Aβ42 (normalized ThT fluorescence); (B) precipitate formation from enantiopure and racemic Aβ(16−22); (C) evolution of rigidity of enantiopure and racemic MAX1 hydrogels; (D) proposed energetics of rippled and pleated sheet formation; (E) evolution of normalized G' under reaction conditions that modulate the energetics of the racemic gel-forming system, and (F) the corresponding fold increase of final G' values. Diagram B reproduced with permission from ref 21. Copyright The Authors, some rights reserved; exclusive licensee MDPI. Distributed under a Creative Commons Attribution License 4.0 (CC BY) https://creativecommons.org/licenses/by/4.0/.

The energy diagram in Figure 14D also predicts that the ability of a racemic mixture to selectively coassemble into rippled sheets (as opposed to self-sort into pleated sheets) should be dependent on the relative activation energies and the total energy available to the system. Figure 14E,F shows an experiment where a racemic mixture of MAX1 and DMAX1 is allowed to assemble into a fibrillar hydrogel under various conditions that modulate either the total energy of the system or the activation energies to effect changes in assembly pathway. Experimentally, this is done by modulating the temperatures and/or the protonation state of the peptide via changes in solution pH. When the energy of the system (E) is greater than the activation energy required to produce rippled fibrils ($\Delta G_{L/D}^{\ddagger}$) but less than the activation energy needed to form enantiomerically pure pleated sheets ($\Delta G_{L}^{\ddagger}$ or $\Delta G_{D}^{\ddagger}$), a large enhancement in the gel's storage modulus (G') is observed

(Figure 14F, blue). Again, this is because stiff fibrils containing only rippled sheets are formed. If the assembly is performed under conditions where the value of E becomes increasingly greater (black and orange data), the overall rate of gelation becomes faster (Figure 14E), but the enhancement in gel rigidity is increasingly diminished. This is presumably because a population of peptides, which increases as E increases, can now self-sort into enantiomerically pure fibrils, which are less stiff.

With respect to thermodynamic stability, Nilsson showed by ITC and sedimentation analysis that the formation of rippled sheets is thermodynamically favored over the pleated alternative (Figure 4 and Figure 14B, respectively).[3,21] Furthermore, Raskatov performed DFT calculations, showing that rippled β-sheets formed by peptides with bulky hydrophobic side chains are favored thermodynamically (Figure 13).[67] The side-chain

packing between sheets is also a consideration when packing sheet interfaces and might prove to be important in designing chiral inhibitors of amyloid formation.[77] However, just like with the kinetic aspects of rippled β-sheet assembly, more work is needed to better understand the thermodynamic parameters associated with those systems.

Lastly, there has been little work done investigating fibril morphology for rippled systems. Polymorphism is indicated by differing appearances of fibrils that arise from the same monomeric constituents.[78] Differences in peptide conformation and packing arrangement within the different fibril types account for polymorphic fibrillar structures.[69] Under appropriate solution conditions, a racemic mixture of peptide should be able to form fibrils containing pleated β-sheets composed exclusively of either all-L or all-D peptides as well as rippled β-sheets composed of alternating L- and D-peptides; each fibril type could have a unique structural morphology, leading to overall polymorphism in the system.

Further, one might envision that "hybrid" fibrils could form where a single fibril might contain segments of rippled and pleated sheets along its fibril length leading to different morphological appearances within a single fiber. Given the complexity of possible assembly outcomes, it is surprising that our laboratories independently observed only the formation of monomorphic rippled fibrils. Although this monomorphic behavior is currently only based on TEM and detailed structural elucidation is needed, it is a provocative thought experiment as to why this might be the case.

The rippled β-sheet is a fascinating structural motif whose characterization lags significantly behind all other folds, although its existence was predicted almost 70 years ago. This unique structure represents an outstanding opportunity for future studies as structural, kinetic, and thermodynamic explorations are just beginning and are currently found predominantly in the context of supramolecular fibrillization. We invite our colleagues in structural biology, protein design/engineering, materials, and other fields to discover the rippled β-sheet and help define and utilize this exciting motif.

■ AUTHOR INFORMATION

Corresponding Authors

Jevgenij A. Raskatov − *Department of Chemistry and Biochemistry, UCSC, Santa Cruz, California 95064, United States;* orcid.org/0000-0002-0082-9113; Email: jraskato@ucsc.edu

Joel P. Schneider − *Chemical Biology Laboratory, Center for Cancer Research, National Cancer Institute, National Institutes of Health, Frederick, Maryland 21702, United States;* Email: joel.schneider@nih.gov

Bradley L. Nilsson − *Department of Chemistry, University of Rochester, Rochester, New York 14627-0216, United States;* orcid.org/0000-0003-1193-3693; Email: bradley.nilsson@rochester.edu

Complete contact information is available at:
https://pubs.acs.org/10.1021/acs.accounts.1c00084

Author Contributions

‖All authors contributed equally.

Notes

The authors declare no competing financial interest.

Biographies

Jevgenij Raskatov studied chemistry at Heideberg University and did his DPhil studies in Organometallics at Oxford University with John Brown. He then went to the California Institute of Technology as a Humboldt Postdoctoral Fellow, to work with Peter Dervan, thus switching fields to Chemical Biology. He has been running an independent laboratory at UCSC since 2014.

Joel Schneider obtained a Ph.D. in chemistry from Texas A&M and did his postdoctoral training at the University of Pennsylvania in protein design. He became full professor at the University of Delaware in 2009 and was subsequently recruited to the NCI, where he currently serves as Chief of the Chemical Biology Laboratory and Deputy Director of Basic Science.

Bradley Nilsson completed a Ph.D. in chemistry at the University of Wisconsin−Madison followed by postdoctoral studies at the University of California, Irvine. He joined the Department of Chemistry at the University of Rochester in 2006, where he has established a research program in peptide supramolecular chemistry and peptide biomaterials.

■ ACKNOWLEDGMENTS

■ DEDICATION

In Memoriam Prof. Joseph F. "Joe" Bunnett, who was the Founding Editor of *Accounts of Chemical Research* at UCSC.

■ REFERENCES

(1) Dutta, S.; Foley, A. R.; Warner, C. J. A.; Zhang, X.; Rolandi, M.; Abrams, B.; Raskatov, J. A. Suppression of Oligomer Formation and Formation of Non-Toxic Fibrils upon Addition of Mirror-Image Aβ42 to the Natural L-Enantiomer. *Angew. Chem., Int. Ed.* **2017**, *56*, 11506−11510.

(2) Nagy, K. J.; Giano, M. C.; Jin, A.; Pochan, D. J.; Schneider, J. P. Enhanced Mechanical Rigidity of Hydrogels Formed from Enantiomeric Peptide Assemblies. *J. Am. Chem. Soc.* **2011**, *133*, 14975−14977.

(3) Swanekamp, R. J.; DiMaio, J. T. M.; Bowerman, C. J.; Nilsson, B. L. Coassembly of Enantiomeric Amphipathic Peptides into Amyloid-Inspired Rippled β-Sheet Fibrils. *J. Am. Chem. Soc.* **2012**, *134*, 5556−5559.

(4) Pauling, L.; Corey, R. B. The Pleated Sheet, a New Layer Configuration of Polypeptide Chains. *Proc. Natl. Acad. Sci. U. S. A.* **1951**, *37*, 251−256.

(5) Pauling, L.; Corey, R. B. Configurations of Polypeptide Chains with Favored Orientations around Single Bonds - Two New Pleated Sheets. *Proc. Natl. Acad. Sci. U. S. A.* **1951**, *37*, 729−740.

(6) Pauling, L.; Corey, R. B. Two Rippled-Sheet Configurations of Polypeptide Chains and a Note about the Pleated Sheets. *Proc. Natl. Acad. Sci. U. S. A.* **1953**, *39*, 253−256.

(7) Lotz, B. Crystal Structure of Polyglycine I. *J. Mol. Biol.* **1974**, *87*, 169−180.

(8) Colonnacesari, F.; Premilat, S.; Lotz, B. Structure of Polyglycine I - Comparison of Antiparallel Pleated and Antiparallel Rippled Sheets. *J. Mol. Biol.* **1974**, *87*, 181−191.

(9) Moore, W. H.; Krimm, S. Vibrational Analysis of Peptide, Polypeptides and Proteins 1. Polyglycine I. *Biopolymers* **1976**, *15*, 2439−2464.

(10) Sakajiri, K.; Kawasaki, E.; Watanabe, J. Distinct complex precipitating from racemic solution of poly(beta-benzyl L-aspartate) and poly(beta-benzyl D-aspartate). *Macromolecules* **2001**, *34*, 7238−7240.

(11) Fuhrhop, J. H.; Krull, M.; Buldt, G. Precipitates with Beta-pleated Sheet Structure by Mixing Aqueous Solutions of Helical Poly(D-Lysine) and Poly(L-Lysine). *Angew. Chem., Int. Ed. Engl.* **1987**, *26*, 699−700.

(12) Rubinstein, I.; Eliash, R.; Bolbach, G.; Weissbuch, I.; Lahav, M. Racemic beta sheets in biochirogenesis. *Angew. Chem., Int. Ed.* **2007**, *46*, 3710−3713.

(13) Weissbuch, I.; Illos, R. A.; Bolbach, G.; Lahav, M. Racemic beta-Sheets as Templates of Relevance to the Origin of Homochirality of Peptides: Lessons from Crystal Chemistry. *Acc. Chem. Res.* **2009**, *42*, 1128−1140.

(14) Wadai, H.; Yamaguchi, K.; Takahashi, S.; Kanno, T.; Kawai, T.; Naiki, H.; Goto, Y. Stereospecific Amyloid-like Fibril Formation by a Peptide Fragment of beta2-Microglobulin. *Biochemistry* **2005**, *44*, 157−164.

(15) Caplan, M. R.; Moore, P. N.; Zhang, S.; Kamm, R. D.; Lauffenburger, D. A. Self-Assembly of a β-Sheet Protein Governed by Relief of Electrostatic Repulsion Relative to van der Waals Attraction. *Biomacromolecules* **2000**, *1*, 627−631.

(16) Bowerman, C. J.; Ryan, D. M.; Nissan, D. A.; Nilsson, B. L. The effect of increasing hydrophobicity on the self-assembly of amphipathic β-sheet peptides. *Mol. BioSyst.* **2009**, *5*, 1058−1069.

(17) Bowerman, C. J.; Liyanage, W.; Federation, A. J.; Nilsson, B. L. Tuning β-Sheet Peptide Self-Assembly and Hydrogelation Behavior by Modification of Sequence Hydrophobicity and Aromaticity. *Biomacromolecules* **2011**, *12*, 2735−2745.

(18) Bowerman, C. J.; Nilsson, B. L. Self-Assembly of Amphipathic β-Sheet Peptides: Insights and Applications. *Biopolymers* **2012**, *98*, 169−184.

(19) Marini, D. M.; Hwang, W.; Lauffenburger, D. A.; Zhang, S.; Kamm, R. D. Left-Handed Helical Ribbon Intermediates in the Self-Assembly of a β-Sheet Peptide. *Nano Lett.* **2002**, *2*, 295−299.

(20) Swanekamp, R. J.; Welch, J. J.; Nilsson, B. L. Proteolytic Stability of Amphipathic Peptide Hydrogels Composed of Self-Assembled Pleated β-Sheet or Coassembled Rippled β-Sheet Fibrils. *Chem. Commun.* **2014**, *50*, 10133−10136.

(21) Urban, J. M.; Ho, J.; Piester, G.; Fu, R.; Nilsson, B. L. Rippled β-Sheet Formation by an Amyloid-β Fragment Indicates Expanded Scope of Sequence Space for Enantiomeric β-Sheet Peptide Coassembly. *Molecules* **2019**, *24*, 1983.

(22) Hule, R. A.; Nagarkar, R. P.; Hammouda, B.; Schneider, J. P.; Pochan, D. J. Dependence of Self-Assembled Peptide Hydrogel Network Structure on Local Fibril Nanostructure. *Macromolecules* **2009**, *42*, 7137−7145.

(23) Rajagopal, K.; Lamm, M. S.; Haines-Butterick, L. A.; Pochan, D. J.; Schneider, J. P. Tuning the pH Responsiveness of beta-Hairpin Peptide Folding, Self-Assembly, and Hydrogel Material Formation. *Biomacromolecules* **2009**, *10*, 2619−2625.

(24) Salick, D. A.; Kretsinger, J. K.; Pochan, D. J.; Schneider, J. P. Inherent antibacterial activity of a peptide-based beta-hairpin hydrogel. *J. Am. Chem. Soc.* **2007**, *129*, 14793−14799.

(25) Schneider, J. P.; Pochan, D. J.; Ozbas, B.; Rajagopal, K.; Pakstis, L.; Kretsinger, J. Responsive hydrogels from the intramolecular folding and self-assembly of a designed peptide. *J. Am. Chem. Soc.* **2002**, *124*, 15030−15037.

(26) Majumder, P.; Zhang, Y.; Iglesias, M.; Fan, L.; Kelley, J. A.; Andrews, C.; Patel, N.; Stagno, J. R.; Oh, B. C.; Furtmüller, G. J.; et al. Multiphase Assembly of Small Molecule Microcrystalline Peptide Hydrogel Allows Immunomodulatory Combination Therapy for Long-Term Heart Transplant Survival. *Small* **2020**, *16*, 2002791.

(27) Branco, M. C.; Pochan, D. J.; Wagner, N. J.; Schneider, J. P. The effect of protein structure on their controlled release from an injectable peptide hydrogel. *Biomaterials* **2010**, *31*, 9527−9534.

(28) Miller, S. E.; Yamada, Y.; Patel, N.; Suàrez, E.; Andrews, C.; Tau, S.; Luke, B. T.; Cachau, R. E.; Schneider, J. P. Electrostatically Driven Guanidinium Interaction Domains that Control Hydrogel-Mediated Protein Delivery In Vivo. *ACS Cent. Sci.* **2019**, *5*, 1750−1759.

(29) Yamada, Y.; Chowdhury, A.; Schneider, J. P.; Stetler-Stevenson, W. G. Macromolecule-Network Electrostatics Controlling Delivery of the Biotherapeutic Cell Modulator TIMP-2. *Biomacromolecules* **2018**, *19*, 1285−1293.

(30) Medina, S. H.; Li, S.; Howard, O. Z.; Dunlap, M.; Trivett, A.; Schneider, J. P.; Oppenheim, J. J. Enhanced immunostimulatory effects of DNA-encapsulated peptide hydrogels. *Biomaterials* **2015**, *53*, 545−553.

(31) Majumder, P.; Baxa, U.; Walsh, S. T.; Schneider, J. P. Design of a Multicompartment Hydrogel that Facilitates Time-Resolved Delivery of Combination Therapy and Synergized Killing of Glioblastoma. *Angew. Chem.* **2018**, *130*, 15260−15264.

(32) Haines-Butterick, L.; Rajagopal, K.; Branco, M.; Salick, D.; Rughani, R.; Pilarz, M.; Lamm, M. S.; Pochan, D. J.; Schneider, J. P. Controlling hydrogelation kinetics by peptide design for three-dimensional encapsulation and injectable delivery of cells. *Proc. Natl. Acad. Sci. U. S. A.* **2007**, *104*, 7791−7796.

(33) Sinthuvanich, C.; Haines-Butterick, L. A.; Nagy, K. J.; Schneider, J. P. Iterative design of peptide-based hydrogels and the effect of network electrostatics on primary chondrocyte behavior. *Biomaterials* **2012**, *33*, 7478−7488.

(34) Yamada, Y.; Patel, N. L.; Kalen, J. D.; Schneider, J. P. Design of a Peptide-Based Electronegative Hydrogel for the Direct Encapsulation, 3D Culturing, in Vivo Syringe-Based Delivery, and Long-Term Tissue Engraftment of Cells. *ACS Appl. Mater. Interfaces* **2019**, *11*, 34688−34697.

(35) Yan, C.; Altunbas, A.; Yucel, T.; Nagarkar, R. P.; Schneider, J. P.; Pochan, D. J. Injectable solid hydrogel: mechanism of shear-thinning and immediate recovery of injectable beta-hairpin peptide hydrogels. *Soft Matter* **2010**, *6*, 5143−5156.

(36) Yan, C.; Mackay, M. E.; Czymmek, K.; Nagarkar, R. P.; Schneider, J. P.; Pochan, D. J. Injectable Solid Peptide Hydrogel as a Cell Carrier: Effects of Shear Flow on Hydrogels and Cell Payload. *Langmuir* **2012**, *28*, 6076−6087.

(37) Marchesan, S.; Waddington, L.; Easton, C. D.; Winkler, D. A.; Goodall, L.; Forsythe, J.; Hartley, P. G. Unzipping the role of chirality in nanoscale self-assembly of tripeptide hydrogels. *Nanoscale* **2012**, *4*, 6752−6760.

(38) Taraban, M. B.; Feng, Y.; Hammouda, B.; Hyland, L. L.; Yu, Y. B. Chirality-Mediated Mechanical and Structural Properties of Oligopeptide Hydrogels. *Chem. Mater.* **2012**, *24*, 2299−2310.

(39) Clover, T. M.; O'Neill, C. L.; Appavu, R.; Lokhande, G.; Gaharwar, A. K.; Posey, A. E.; White, M. A.; Rudra, J. S. Self-Assembly of Block Heterochiral Peptides into Helical Tapes. *J. Am. Chem. Soc.* **2020**, *142*, 19809−19813.

(40) Nagy-Smith, K.; Moore, E.; Schneider, J.; Tycko, R. Molecular structure of monomorphic peptide fibrils within a kinetically trapped hydrogel network. *Proc. Natl. Acad. Sci. U. S. A.* **2015**, *112*, 9816−9821.

(41) Micklitsch, C. M.; Medina, S. H.; Yucel, T.; Nagy-Smith, K. J.; Pochan, D. J.; Schneider, J. P. Influence of hydrophobic face amino acids on the hydrogelation of β-hairpin peptide amphiphiles. *Macromolecules* **2015**, *48*, 1281−1288.

(42) Nagy-Smith, K.; Beltramo, P. J.; Moore, E.; Tycko, R.; Furst, E. M.; Schneider, J. P. Molecular, Local, and Network-Level Basis for the Enhanced Stiffness of Hydrogel Networks Formed from Coassembled Racemic Peptides: Predictions from Pauling and Corey. *ACS Cent. Sci.* **2017**, *3*, 586−597.

(43) Mackintosh, F. C.; Kas, J.; Janmey, P. A. Elasticity of Semiflexible Biopolymer Networks. *Phys. Rev. Lett.* **1995**, *75*, 4425−4428.

(44) Morse, D. C. Viscoelasticity of concentrated isotropic solutions of semiflexible polymers. 1. Model and stress tensor. *Macromolecules* **1998**, *31*, 7030−7043.

(45) Morse, D. C. Viscoelasticity of concentrated isotropic solutions of semiflexible polymers. 2. Linear response. *Macromolecules* **1998**, *31*, 7044−7067.

(46) Wouters, M. A.; Curmi, P. M. G. An analysis of side chain interactions and pair correlations within antiparallel β-sheets: The differences between backbone hydrogen-bonded and non-hydrogen-bonded residue pairs. *Proteins: Struct., Funct., Genet.* **1995**, *22*, 119−131.

(47) Raskatov, J. A. Chiral Inactivation: an Old Phenomenon with a New Twist. *Chem. - Eur. J.* **2017**, *23*, 16920−16923.

(48) Foley, A. R.; Raskatov, J. A. Understanding and controlling amyloid aggregation with chirality. *Curr. Opin. Chem. Biol.* **2021**, *64*, 1.

(49) Jacques, J.; Collet, A.; Wilen, S. H. *Enantiomers, racemates, and resolutions;* Wiley: New York, 1991.

(50) Raskatov, J. A.; Thompson, A. L.; Cowley, A. R.; Claridge, T. D. W.; Brown, J. M. Chiral recognition in contact ion-pairs; observation, characterization and analysis. *Chem. Sci.* **2013**, *4*, 3140−3147.

(51) Raskatov, J. A.; Jakel, M.; Straub, B. F.; Rominger, F.; Helmchen, G. Iridium-Catalyzed Allylic Substitutions with Cyclometalated Phosphoramidite Complexes Bearing a Dibenzocyclooctatetraene Ligand: Preparation of (pi-Allyl)Ir Complexes and Computational and NMR Spectroscopic Studies. *Chem. - Eur. J.* **2012**, *18*, 14314−14328.

(52) Selkoe, D. J.; Hardy, J. The amyloid hypothesis of Alzheimer's disease at 25 years. *EMBO Mol. Med.* **2016**, *8*, 595−608.

(53) Chiti, F.; Dobson, C. M. Protein misfolding, functional amyloid, and human disease. *Annu. Rev. Biochem.* **2006**, *75*, 333−366.

(54) Walsh, D. M.; Lomakin, A.; Benedek, G. B.; Condron, M. M.; Teplow, D. B. Amyloid beta-protein fibrillogenesis - Detection of a protofibrillar intermediate. *J. Biol. Chem.* **1997**, *272*, 22364−22372.

(55) Ono, K.; Condron, M. M.; Teplow, D. B. Structure-neurotoxicity relationships of amyloid beta-protein oligomers. *Proc. Natl. Acad. Sci. U. S. A.* **2009**, *106*, 14745−14750.

(56) Bitan, G.; Kirkitadze, M. D.; Lomakin, A.; Vollers, S. S.; Benedek, G. B.; Teplow, D. B. Amyloid beta-protein (A beta) assembly: A beta 40 and A beta 42 oligomerize through distinct pathways. *Proc. Natl. Acad. Sci. U. S. A.* **2003**, *100*, 330−335.

(57) Foley, A. R.; Lee, H.-W.; Raskatov, J. A. A Focused Chiral Mutant Library of the Amyloid β 42 Central Electrostatic Cluster as a Tool to Stabilize Aggregation Intermediates. *J. Org. Chem.* **2020**, *85*, 1385−1391.

(58) Foley, A. R.; Finn, T. S.; Kung, T.; Hatami, A.; Lee, H.-W.; Jia, M.; Rolandi, M.; Raskatov, J. A. Trapping and Characterization of Nontoxic Aβ42 Aggregation Intermediates. *ACS Chem. Neurosci.* **2019**, *10*, 3880−3887.

(59) Warner, C. J. A.; Dutta, S.; Foley, A. R.; Raskatov, J. A. Introduction of D-glutamate at a critical residue of Aβ42 stabilizes a prefibrillary aggregate with enhanced toxicity. *Chem. - Eur. J.* **2016**, *22*, 11967−11970.

(60) Ahmed, M.; Davis, J.; Aucoin, D.; Sato, T.; Ahuja, S.; Aimoto, S.; Elliott, J. I.; Van Nostrand, W. E.; Smith, S. O. Structural conversion of neurotoxic amyloid-beta(1−42) oligomers to fibrils. *Nat. Struct. Mol. Biol.* **2010**, *17*, 561−U56.

(61) Urbanc, B.; Cruz, L.; Yun, S.; Buldyrev, S. V.; Bitan, G.; Teplow, D. B.; Stanley, H. E. In silico study of amyloid beta-protein folding and oligomerization. *Proc. Natl. Acad. Sci. U. S. A.* **2004**, *101*, 17345−50.

(62) Gremer, L.; Schölzel, D.; Schenk, C.; Reinartz, E.; Labahn, J.; Ravelli, R. B. G.; Tusche, M.; Lopez-Iglesias, C.; Hoyer, W.; Heise, H.; Willbold, D.; Schröder, G. F. Fibril structure of amyloid-β(1−42) by cryo−electron microscopy. *Science* **2017**, *358*, 116−119.

(63) Dutta, S.; Rodriguez Foley, A.; Kuhn, A.; Abrams, B.; Lee, H.-W.; Raskatov, J. A. New insights into differential aggregation of enantiomerically pure and racemic Aβ40 systems. *Peptide Sci.* **2019**, *111*, e24139.

(64) Ghanta, J.; Shen, C.-L.; Kiessling, L. L.; Murphy, R. M. A Strategy for Designing Inhibitors of β-Amyloid Toxicity. *J. Biol. Chem.* **1996**, *271*, 29525−29528.

(65) Chalifour, R. J.; McLaughlin, R. W.; Lavoie, L.; Morissette, C.; Tremblay, N.; Boule, M.; Sarazin, P.; Stea, D.; Lacombe, D.; Tremblay, P.; Gervais, F. Stereoselective interactions of peptide inhibitors with the beta-amyloid peptide. *J. Biol. Chem.* **2003**, *278*, 34874−34881.

(66) Raskatov, J. A. Conformational Selection as the Driving Force of Amyloid β Chiral Inactivation. *ChemBioChem* **2020**, *21*, 2945−2949.

(67) Raskatov, J. A. A DFT study of structure and stability of pleated and rippled cross-β sheets with hydrophobic sidechains. *Biopolymers* **2021**, *112*, e23391.

(68) Qiang, W.; Yau, W.-M.; Luo, Y.; Mattson, M. P.; Tycko, R. Antiparallel β-sheet architecture in Iowa-mutant β-amyloid fibrils. *Proc. Natl. Acad. Sci. U. S. A.* **2012**, *109*, 4443−4448.

(69) Foley, A. R.; Raskatov, J. A. A DFT-assisted topological analysis of four polymorphic, S-shaped Aβ42 fibril structures. *ChemBioChem* **2019**, *20*, 1722−1724.

(70) Chiti, F.; Dobson, C. M. Protein misfolding, amyloid formation, and human disease: a summary of progress over the last decade. *Annu. Rev. Biochem.* **2017**, *86*, 27−68.

(71) Eichner, T.; Radford, S. E. A diversity of assembly mechanisms of a generic amyloid fold. *Mol. Cell* **2011**, *43*, 8−18.

(72) Chatani, E.; Yamamoto, N. Recent progress on understanding the mechanisms of amyloid nucleation. *Biophys. Rev.* **2018**, *10*, 527−534.

(73) Dear, A. J.; Michaels, T. C.; Meisl, G.; Klenerman, D.; Wu, S.; Perrett, S.; Linse, S.; Dobson, C. M.; Knowles, T. P. Kinetic diversity of amyloid oligomers. *Proc. Natl. Acad. Sci. U. S. A.* **2020**, *117*, 12087−12094.

(74) Linse, S. Monomer-dependent secondary nucleation in amyloid formation. *Biophys. Rev.* **2017**, *9*, 329−338.

(75) Collins, S. R.; Douglass, A.; Vale, R. D.; Weissman, J. S. Mechanism of prion propagation: amyloid growth occurs by monomer addition. *PLoS Biol.* **2004**, *2*, e321.

(76) Cannon, M. J.; Williams, A. D.; Wetzel, R.; Myszka, D. G. Kinetic analysis of beta-amyloid fibril elongation. *Anal. Biochem.* **2004**, *328*, 67−75.

(77) Torbeev, V.; Grogg, M.; Ruiz, J.; Boehringer, R.; Schirer, A.; Hellwig, P.; Jeschke, G.; Hilvert, D. Chiral recognition in amyloid fiber growth. *J. Pept. Sci.* **2016**, *22*, 290−304.

(78) Tycko, R. Amyloid Polymorphism: Structural Basis and Neurobiological Relevance. *Neuron* **2015**, *86*, 632−645.